

Cyanobacteria alter lipid metabolism in zooplankton via exudates of obesogens

Jinlong Zhang^{a,1}, Xuexiu Chang^{b,c,1}, Hugh J. MacIsaac^{a,c}, Yuan Zhou^{b,d}, Daochun Xu^a, Jingjing Li^b, Jun Xu^a, Tao Wang^a, Hongyan Zhang^a, Zimeng Peng^a, Jiayao Wen^a, Runbing Xu^{a,*}

^a Yunnan Key Laboratory for Plateau Mountain Ecology and Restoration of Degraded Environments, School of Ecology and Environmental Science, Yunnan University, Kunming 650091, China

^b Yunnan Collaborative Innovation Center for Plateau Lake Ecology and Environmental Health, College of Agronomy and Life Sciences, Kunming University, Kunming 650214, China

^c Great Lakes Institute for Environmental Research, University of Windsor, Windsor, ON N9B 3P4, Canada

^d The Ecological and Environmental Monitoring Station of DEEY in Kunming, Kunming 650228, China

ARTICLE INFO

Keywords:

Microcystis aeruginosa
Triacylglycerol
Glycerol tristearate
Daphnia magna
Fat metabolism

ABSTRACT

Lipid metabolism of zooplankton plays an important role in aquatic food web, however, is threatened by abiotic and biotic factors. Recently blooming cyanobacteria providing low-quality food for zooplankton, have been found to be a potential source of lipid metabolism disorder and reproductive disturbance in aquatic animals, though mechanisms of operation are unclear. Here we assessed effects of cyanobacterial exudates on lipid metabolism and reproduction in *Daphnia magna*. *Microcystis aeruginosa* exudates (MaE, 2×10^4 cells/mL and 4×10^5 cells/mL) induced increased lipid droplets and altered lipid components in exposed *Daphnia*. MaE activated ecdysone and juvenile hormone signaling pathways by increasing hormone content and activities of ecdysone receptor and steroid receptor coactivator, which stimulated sterol regulatory element binding protein to increase lipid accumulation. MaE also increased expression of *ECR*, *HR3*, *Neverland* and *RXR* genes in the ecdysone pathway, *Met* and *SRC* genes in the juvenile hormone pathway, and *SREBP-1* and *DGAT-1* genes in the triacylglycerol (TAG) synthesis pathway. The increase in lipid production promoted both reproduction and growth of *Daphnia*. Glycerol tristearate (GTS, a TAG lipid species) in MaE solutions was positively correlated with cholesterol, TAG, and reproductive hormones in exposed *Daphnia*. Disordered lipid metabolism of zooplankton caused by cyanobacteria exudates is consistent with obesogen hypothesis (Baillie-Hamilton, 2002) and poses a risk to aquatic ecosystems.

1. Introduction

Zooplankton like *Daphnia* play pivotal roles in aquatic food web, grazing on high-quality phytoplankton with polyunsaturated fatty acids (PUFAs) and transferring these energy-rich nutrients to higher trophic levels (De Meester et al., 2023). Thus, fat metabolism is an important physiological process of zooplankton, which is not only the cornerstone of energy metabolism, growth and development of these primary consumers, but in turn is also a key aspect of material conversion and energy transfer in aquatic ecosystems (Catala, 2013; Lynn et al., 2015). Recently, some pollutants - industrial chemicals or hormone drugs

including ecdysteroids, juvenoids, tributyltin and bisphenol A - increase accumulation of storage lipids such as triacylglycerols (TAG) and cholesterol into lipid droplets in *Daphnia magna*, a invertebrate example of the lipidic disruption phenomenon (Fuentes et al., 2018; Jordão et al., 2016a; Jordão et al., 2015; Jordão et al., 2016b). These xenobiotic chemicals have been termed 'obesogens' or metabolic disruptors owing to their ability to interfere with lipid allocation in vertebrates and causing obesity and related metabolic disorders (Baillie-Hamilton, 2002; Grün and Blumberg, 2009). Besides those abiotic obesogens, fat metabolism of zooplankton is possibly threatened by biotic factors, such as blooming cyanobacteria. Zhou et al. (2023) classified 155 lipids from

* Corresponding author.

E-mail address: runbingxu@ynu.edu.cn (R. Xu).

¹ Jinlong Zhang and Xuexiu Chang contributed equally to this work.

<https://doi.org/10.1016/j.hal.2024.102790>

Received 3 September 2024; Received in revised form 18 December 2024; Accepted 19 December 2024

Available online 1 January 2025

1568-9883/© 2024 Elsevier B.V. All rights are reserved, including those for text and data mining, AI training, and similar technologies.

the 409 total metabolites identified in exudates of *Microcystis aeruginosa*, one of the most dominant species of cyanobacteria bloom worldwide. Among those lipids in *M. aeruginosa* exudates, phytosphingosine, a sphingolipid induced immunotoxicity, oxidative stress and inflammatory responses in fish (Li et al., 2024; Zhao et al., 2023). Wang et al. (2024) also observed that exudates of both toxic strains and non-toxic strains of *Microcystis* induced TAG production of *D. magna*. Yet, whether these cyanobacterial extracellular compounds can affect lipid metabolism of zooplankton is unclear. Both frequency and size of cyanobacterial blooms are increasing globally due to the intensifying eutrophication and global warming (Ho et al., 2019; Paerl and Huisman, 2008), posing growing threats to both aquatic life and human health (Huisman et al., 2018; Plaas and Paerl, 2021). Thus, identification of the presence and roles of cyanobacterial obesogens has become a crucial problem.

In contrast to high quality phytoplankton blooms transferring primary products to higher trophic levels, cyanobacterial blooms can only provide poor food for animals due to their lack of sterols and most essential lipids for zooplankton (Dickman et al., 2008; Thomas et al., 2022), large colonial or filamentous morphology hindering filtration processes of grazers (Lürding, 2021), and toxicity caused by large amounts of secondary metabolites (Jones et al., 2021). In particular, when *Daphnia* encounters toxic or filamentous algae in its filter comb, it ejects all collected particles – including nutritious prey – and may even stop grazing until finding a more suitable prey community (DeMott et al., 2001; DeMott et al., 1991). As a result of these, cyanobacteria may negatively affect the co-existing zooplankton mainly by releasing extracellular secondary metabolites into water instead of being ingested by these primary consumers. In previous studies, while many cyanotoxins, such as microcystins (MCs), exhibit negative effects on growth and reproduction of zooplankton (Ger et al., 2016; Lürding and van der Grinten, 2003), other extracellular chemicals have been isolated from cyanobacteria cultures and proved to do harm to zooplankton and other aquatic animals, e.g., phytosphingosine (Zhao et al., 2023) and volatile organic compounds (VOCs), with representation of β -cyclocitral (Chen et al., 2024; Zuo, 2023). However, whether the lipids included in cyanobacterial secondary metabolites are responsible for their harm to zooplankton remains unknown.

D. magna is often used as a model species in ecotoxicology owing to its fast reproduction, short generation time, easy culturing, and its stress sensitivity (e.g. Flaherty and Dodson (2005)). Also, previous studies have developed referenceable tools such as lipid droplet staining and lipidomic analysis for observing lipid accumulation and changes in *D. magna* exposed to abiotic obesogens (Fuertes et al., 2019; Fuertes et al., 2020; Jordão et al., 2015; Sengupta et al., 2017). The purpose of this study was to examine the fat metabolism response of *D. magna* to exudates of *M. aeruginosa* (MaE), and to explore the mechanism of fat metabolism disturbance and its effect on reproductive efficiency. Accordingly, we assessed changes in lipid droplet accumulation, lipid profiles, TAG biosynthesis, reproduction characteristics, and expression of genes involved in lipid metabolism and reproduction in *D. magna*.

2. Materials and methods

2.1. Algae culture and *M. aeruginosa* exudates (MaE) preparation

M. aeruginosa (FACHB-905) and *Chlorella vulgaris* (FACHB-32) were purchased from the Freshwater Algae Culture Collection of the Institution of Hydrobiology at the Chinese Academy of Sciences. Both species were cultured axenically with HGZ-145 medium and COMBO medium, respectively, in an artificial climate chamber (LRH-400-GSI) at 25 ± 1 °C, with a light: dark photoperiod of 12:12 h, and a luminous flux of 120 $\mu\text{mol photons m}^{-2}\text{s}^{-1}$ measured by a quantum meter (Spectrum Technology, Inc., USA). Cultures of algae were manually shaken three times per day. Density of algae was counted manually using a hemocytometer under an optical microscope (OLYMPUS-BX43, Japan) every day during

the culture period.

M. aeruginosa was cultured to the exponential growth phase, then axenically inoculated in fresh medium at two different initial densities: 1×10^4 cells/mL and 2×10^5 cells/mL, with target values of 2×10^4 cells/mL and 4×10^5 cells/mL, respectively, based on previous studies (Xu et al., 2019). The two solutions of *M. aeruginosa* cells (2.0×10^4 cells/mL and 4×10^5 cells/mL) were centrifuged at 4 °C for 10min at 6000 r/min. Supernatant was filtered through a 0.22 μm glass fiber filter (MiLiMo separation technology limited company, Shanghai) to obtain the MaE solution. MaE solutions were kept at 4 °C until a few hours just before use.

2.2. *Daphnia magna* cultivation

D. magna was originally obtained from Guangdong Laboratory Animal Monitoring Institute (Guangzhou, China), and grown for more than three generations in the laboratory (Kunming, China) at 25 °C under a constant 12:12 h light: dark cycle. Each 10 individuals of *D. magna* were cultured in a glass beaker containing 500 mL COMBO medium, and fed with 5×10^5 cells/mL of *C. vulgaris* every day. The culture solution was updated three times per week. Healthy *D. magna* bearing eggs were selected and fed with same *C. vulgaris* cell density to produce neonates. Newborns (<24 h) from the third or fourth brood were selected for exposure experiments owing to their stable parthenogenetic reproduction.

2.3. Experimental design

Chronic and acute toxicity tests were performed by exposing *D. magna* to COMBO medium with: (1) a control treatment without MaE (Control); (2) *M. aeruginosa* exudates of low cell density (2.0×10^4 cells/mL; Low MaE); or (3) high cell density (4×10^5 cells/mL; High MaE).

Experiment 1 was an acute exposure test to determine the effects of MaE on lipid droplet accumulation, the synthesis of lipids including TAG, the selected major genes, and lipid dynamics in *D. magna*. This experiment was carried out in a 500 mL beaker. Two hundred young (<24 h) *Daphnia* individuals were cultured with 400 mL of experimental solution with five replicates for each treatment (200 individuals \times 4 replicates), for 48 h and 96 h, respectively. We fed daphnids daily to ensure adequate nutrition (5×10^5 cells/mL of *C. vulgaris*), refreshed the medium daily, and removed the shell from the body of daphnids. In order to obtain samples for enzyme-linked immunosorbent assay, gene transcription and lipidomics, we performed three independent experiments in parallel. All replicates of each treatment were collected after 48 h and 96 h, respectively, frozen in liquid nitrogen and stored at -80 °C for subsequent measurement.

Experiment 2 consisted of a chronic toxicity test to explore the effects of MaE on reproductive development. Animals were exposed to the above three different solutions for 21 days. Exposure was carried out in a 100 mL glass beaker containing 50 mL of the solution of each treatment, with a single newborn (<24 h) placed in each beaker, with ten replicates for each treatment. Daphnids were fed daily (5×10^5 cells/mL of *C. vulgaris*) and the test solution was refreshed daily. Survival, growth and reproduction of *D. magna* were recorded daily as number of molts per individual, days to first brood, days to first egg production, number of eggs in first brood, and the total number of molts per individual. Body length (from the head to the bottom of the thorn) of each mother was measured on the 7st, 14st and 21st day with a stereo microscope and micrometer.

2.4. Nile red determination

Methods followed previous studies (Jordão et al., 2016a, 2015) with slight modification. Briefly, ten animals of each treatment were randomly collected from the acute exposure test (Experiment 1) after 48 h and 96 h, and lipid droplets were quantitatively analyzed using Nile

Red (Sigma). Nile red stock solution was prepared in acetone and stored in dark. Before use, it was diluted to 1.5 μM with COMBO medium to obtain the working solution. *D. magna* was exposed to the Nile red solution at 20 °C for 1 h without light. Stained *D. magna* was placed in 100 mL COMBO medium for 1 min to remove Nile Red residue. Subsequently, each individual was placed in a 1.5 mL EP centrifuge tube to remove residual liquids, and then 300 μM isopropanol was added and ultrasonically broken. 200 μL of supernatant was centrifuged at 10,000 g for 15 min, and fluorescence intensity of Nile red measured with a fluorescence microplate reader (Synergy 2, BioTek, USA) at a wavelength of 530/590 nm. 10 individuals of *D. magna* in each treatment were used for measurement, while 10 controls not exposed to Nile red were used as background fluorescence references. Nile red fluorescence images were captured under an inverted fluorescence microscope (Nikon SMZ1500, Japan) with GFP filter (EX472/30, EM520/35).

2.5. Enzyme-linked immunosorbent assays

We measured performance of hormone synthesis of *D. magna* by using commercial ELISA kit (Jiangsu Kot, China) and microtiter plate reader (Lab Systems Multiskan® MS, Finland). We measured the following parameters: content of TAG, cholesterol, ecdysone, 20-hydroxyecdysone and juvenile hormone involved in the synthesis of TAG, and activities of ecdysterone 2-hydroxylase (E2H), ecdysone 20-monooxygenase (CYP314A1), farnesic acid methyltransferase (FAMeT), ECR, retinoic acid X receptor (RXR), steroid receptor coactivator (SRC), sterol regulatory element binding protein (SREBP), acetyl-CoA carboxylase (ACC) and diacylglycerol acyltransferase (DGAT).

2.6. Total RNA isolation and real-time qPCR

Total RNA was isolated from daphnids using RNAisoPlus reagent (Takara, Japan) according to manufacturer's instructions. After isolation, the concentration and purity of RNA were detected using an ultratrace nucleic acid analyzer (ScanDrop 100, Analytik Jena, Germany). Following this, we diluted RNA samples with RNase-free H₂O to keep consistent concentrations. We conducted reverse transcription using a TURScript 1st Stand cDNA SYNTHESIS Kit (Aidlab Company) according to the manufacturer's protocol, while cDNA was obtained for *D. magna* in each treatment.

Primers were designed for quantitative real-time polymerase chain reaction (RT-qPCR) according to known sequences listed in Table S1, where the *G3DPH* gene was used as an internal standard and the other nine genes used to analyze expression in *D. magna* after exposure to MaE. Primers of most genes were designed according to previous studies (Jordão et al., 2015) while those of *SREBP-1* and *DGAT-1* were designed using Primer 5. qPCR experiment was conducted using an qTOWER2.2 fluorescence quantitative PCR instrument (Analytik Jena AG, Germany) based on the detection of the ordinary PCR instrument analytikjena-Easycycler (Germany) system. The initial denaturation thermal cycle was carried out at 95 °C for 3 min, and then 39 cycles were repeated at 95 °C for 5 s, finally 30 s were repeated at 60 °C to quantify the relative expression of each gene. The relative expression of each gene was calculated by the $2^{-\Delta\Delta\text{Ct}}$ method (Schmittgen and Livak, 2008).

2.7. Lipidomic analysis

D. magna samples (50 mg) of each treatment were mixed with 500 μL of precooled buffer solution (methyl tert-butyl ether: methanol = 5: 1, v/v) at -20 °C. Samples were then treated with a 45 Hz grinder for 12 min, followed by vortex mixing for 30 s and ultrasonic treatment for 15 min. Samples were then placed at -40 °C for 1 h. After centrifugation and freeze-drying, the sample was redissolved with 200 μL (dichloromethane: methanol = 1: 1, v/v) solution and centrifuged again. Finally, 5 μL of each sample was used for lipid detection. Equal amount of

solution was mixed from each sample to form QC sample. Treatments were replicated three times.

We used UPLC equipment equipped with an ACQUITY UPLC CSH C18 column (100 × 2.1 mm, 1.7 μm , Waters, MA, USA) for separation. The temperature of chromatographic column was maintained at 55 °C, and the flow rate was controlled at 400 $\mu\text{L}/\text{min}$. mobile phase A was composed of acetonitrile: water (60:40, v/v), 10mM ammonium acetate and 0.1 % formic acid; mobile phase B was composed of isopropanol: water (90:10, v/v), acetonitrile solution, 10 mM ammonium acetate and 0.1% formic acid. Gradient elution was performed under the following conditions: 0–2min, B phase 40–43 %; 2–12 min, B phase 50–54 %; 12–18min, B phase 70–99 %; 18–20 min, B phase 40 %. The MSE mode controlled by MassLynx V4.2 (Waters) was used for primary and secondary mass spectrometry data acquisition by Watschw Xevo G2-XS QToF high resolution mass spectrometer (USA). The scanning range of TOF mass in the first stage was 100–2000 Da in the positive mode and 50–2000 Da in the negative mode. For MS/MS detection, parent ions were fragmented at 10–40 eV.

Raw data collected using MassLynx V4.2 was processed by Progenesis QI software for peak extraction, peak alignment and other data processing operations, based on the Progenesis QI software online METLIN database and Biomark's self-built library for identification. At the same time, theoretical fragment was identified and mass deviation determined; all were within 100 ppm.

Principal component analysis and Spearman correlation analysis were used to assess repeatability of samples within treatments and the quality of control samples. Identified compounds were searched for classification and pathway information in KEGG, HMDB and lipidmaps databases.

2.8. TAG lipid species in *M. aeruginosa* exudates

Based on a list of lipids obtained from lipidomic analysis on *M. aeruginosa* exudates (Unpublished Data), we purchased three chemicals - glycerol tristearate (GTS, CAS no.555-43-1, C₅₇H₁₁₀O₆, MW: 891.48), trilaurin (CAS no.538-24-9, C₃₉H₇₄O₆, MW: 639.00) and tritridecanoin (CAS no.555-45-3, C₄₅H₈₆O₆, MW: 723.16), from Yuanye Bio-Technology (Shanghai, China). The determination and optimization of these chemicals contained in MaE solutions were conducted using an Agilent 1290 Infinity II Bio LC coupled to an Agilent 6475 LC/TQ system (Agilent Technologies, Inc., CA, USA) via multiple reaction monitoring, following internal methods provided by Agilent Technologies with slight modifications. In short, all lipid standards were combined and diluted with isopropanol to a final working solution. Sample separation was performed using the Agilent 1290 Infinity II Bio LC system. The mobile phase A consisted of water: acetonitrile: isopropanol (50:30:20, v/v/v) and 10 mmol/L ammonium formate. The mobile phase B consisted of water: acetonitrile: isopropanol (1:9:90, v/v/v) and 10 mmol/L ammonium formate. The auto-sampler temperature was 4 °C and column temperature was 40 °C, and the injection volume was 2 μL . The gradient profile used was 15–50 % B in 1.5 min, 50–70 % B in 3 min, 70–90 % B in 1 min, 100–15 % B in 0.5 min, 15 % B in 2 min. Mass spectrometric analysis was performed using Agilent 6475 LC/TQ system. Lipid classes were quantified using the following ion forms: [M + NH₄]⁺ for GTS, trilaurin and tritridecanoin. Source and gas setting were as follow: Gas temperature = 300 °C, Dry gas flow = 13 L/min, Sheath gas flow = 11 L/min, Sheath gas temperature = 250 °C, Nebulizer = 35 psi, Capillary voltage = 4000 V (+). Quantitation was performed using external calibration curves with 1/x weighting. The retention time of each analyte peak to the average of standard peaks was within ± 0.15 min, and the ion ratio was within the tolerance of 30 %.

2.9. Statistical analysis

Data were checked for normality and homogeneity of variance using SPSS Statistics 25.0 software. One-way analysis of variance (ANOVA)

and Tukey HSD test were used to evaluate differences between controls and treatments. The rejection level was set at $\alpha < 0.05$. We present experimental data as mean \pm standard deviation. After lipidomic analysis, we used a *t*-test to calculate the difference significance *P* value of each compound. We used the R language package ropls to perform OPLS-DA modeling, and 200 times permutation tests were performed to verify reliability of the model. Screening criteria used for differential metabolites were $FC > P \text{ value} < 0.05$ and $VIP > 1$. The significance of differences among difference metabolites of KEGG pathway enrichment were calculated using a hypergeometric distribution test.

3. Results

3.1. Lipid storage in *Daphnia* exposed to MaE

Analysis of fat content using Nile Red staining revealed that fluorescence levels in *D. magna* were higher in the high and low MaE treatments than in the control at both 48 h and 96 h (Fig. 1A). After 48 h exposure, elevated fluorescence levels were observed only in the high MaE treatment relative to the control (Figure 1B, $P < 0.05$). After 96 h of exposure, fluorescence levels were significantly higher in both MaE treatments relative to the control, and the high density MaE treatment was significantly greater than the low density MaE treatment (Fig. 1B, $P < 0.05$).

3.2. Lipid metabolites of *Daphnia* exposed to MaE

Lipid metabolite profiles of *D. magna* changed significantly after exposure to MaE (Figure S1). After 48 h exposure to low density MaE and high density MaE treatments, 472 and 748 lipid metabolites were up-regulated, whereas 141 and 752 lipid metabolites were down-regulated groups, respectively, all relative to the control (Figure S2-A and Supplementary Material). Similarly, 68 and 642 lipid metabolites were up-regulated while 56 and 592 lipid metabolites were down-regulated in low density MaE and high density MaE treatments, respectively (see Fig. S2-B and Supplementary Material). We classified measured lipid metabolites into eight categories: fatty acyl (FA), glycerolipids (GI), glycerophospholipids (GP), sphingolipids (SP), sterol lipids (ST), polyketides (PK), prenol lipids (PR) and saccharolipids (SL). After 48 h exposure, we observed 210 up-regulated and 68 down-regulated metabolites from these categories in the low density MaE treatment (compared with the control) (Fig. 2A). In the high density

MaE treatment, only GI metabolites were more up- than down-regulated, whereas the other seven lipid categories were all more down- than up-regulated (Fig. 2B). After 96 h exposure, GL, GP, SP, ST and PK lipid metabolites in the low density MaE treatment were more up- than down-regulated relative to the control, while the opposite was true for FA and PR metabolites (Fig. 2C). In the high density MaE treatment, only GP and SP metabolites were more up- than down-regulated, while the remaining six categories of lipids were mainly down-regulated (Fig. 2D).

After 48 h exposure, Lipidmaps software found that, the low density MaE treatment had more up- than down-regulated metabolites of fatty acids, TAG, DAG, PC, PA, PE, SM, Cer, Sterol and CE relative to controls, while down-regulated metabolites were more common only for PS, PG and PI (Table 1). In the high density MaE treatment, up-regulated metabolites of TG, DG, PC, PA, PE, Sterol and CE exceeded those that were down-regulated, and down-regulated metabolites were more common only for PS, PG, PI and Cer.

After 96 h exposure, the low density MaE treatment had more metabolites of TG, PC, PS, PE, Cer, Sterol and CE that were up- than down-regulated relative to the control, and only fatty acid, PA and PI were more down- than up-regulated. In the high MaE treatment at 96 h, more metabolites of PC, PA, PS, PE and Cer were up- than down-regulated, while fatty acid, DG, PG, PI, Sterol and CE were more commonly down- than up-regulated (Table 1). Collectively, these results demonstrate that MaE increased the content of TAG in *D. magna* following acute exposure.

We annotated the KEGG pathway of differential lipid metabolites in *D. magna* after acute exposure to MaE and identified the dominant enrichment pathway. Following 48 h exposure, the low density MaE treatment did not induce significant enrichment of differential metabolites, whereas the high density MaE treatment resulted in down-regulation of the sphingolipid signaling pathway, the neurotrophin signaling pathway, the adipocytokine signaling pathway, the AGE-RAGE signaling pathway, and the insulin resistance pathway (Fig. 3). When exposure time was increased to 96 h, the low density MaE treatment up-regulated fat digestion and absorption, whereas six metabolic pathways were down-regulated including the calcium signaling pathway and steroid biosynthesis (Fig. 3). The high density MaE treatment induced up-regulation of inflammatory mediator regulation of TRP channels, while down-regulating the target pathway of serotonergic synapses.

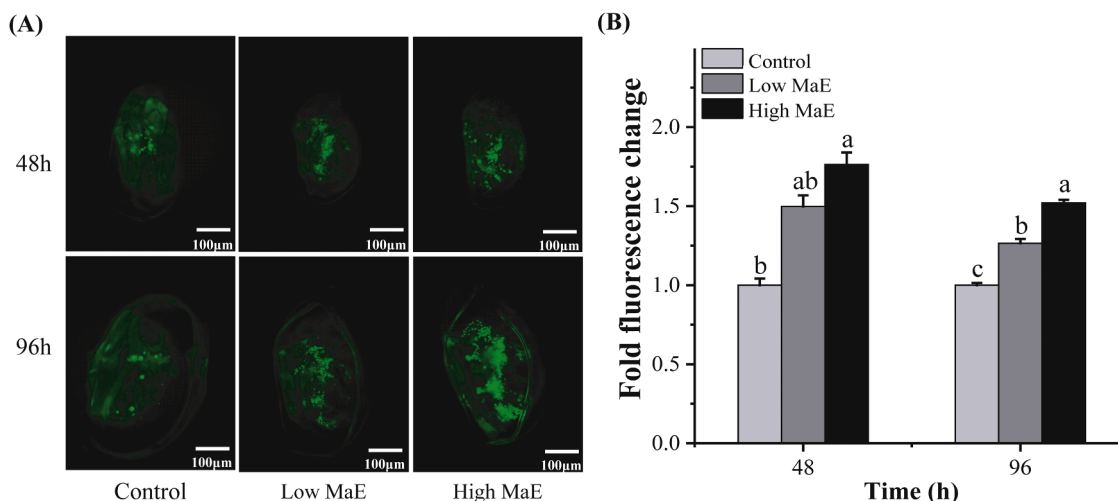


Fig. 1. Qualitative and quantitative evaluation of fat stored in *D. magna* (Low density MaE: exudates from 2×10^4 cells/mL; High density MaE: exudates from 4×10^5 cells/mL). (A) Fluorescence microscopy of lipid accumulation in individual daphnids following 48 h and 96 h exposure to different MaE density treatments. (B) Fluorescence levels in *D. magna* at 48 h and 96 h under control, or low or high cell density MaE. Error bars indicate standard deviation of the mean (SD) ($n=10$ replicates). Different letters on the bars indicate significant differences between the treatments using one-way ANOVA (Tukey HSD, $P < 0.05$).

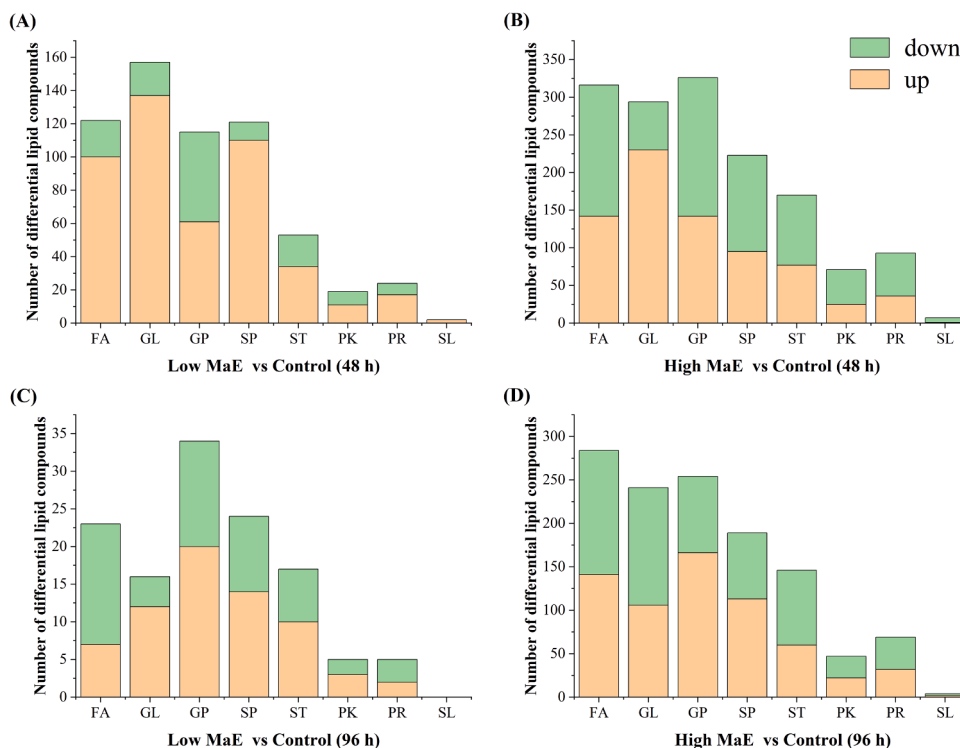


Fig. 2. Up-regulation and down-regulation of major lipid metabolites in *D. magna* after acute exposure to MaE at different cell densities (n = 3) for 48 h (upper panels) or 96 h (lower panel).

Table 1
Changes of key lipids associated with reproduction in *Daphnia* (Numbers in the table are number of lipid species).

Lipid metabolites	Low MaE vs Control (48 h)		High MaE vs Control (48 h)		Low MaE vs Control (96 h)		High MaE vs Control (96 h)	
	up	down	up	down	up	down	up	down
Fatty acid	74	24	148	148	9	13	130	142
Triacylglycerol (TAG)	95	18	149	29	10	2	69	87
Diacylglycerol (DAG)	27	1	60	24	1	1	27	41
Phosphatidyl choline (PC)	11	1	20	14	4	2	32	6
Phosphatidic acid (PA)	6	1	9	8	0	2	13	6
Phosphatidylserine (PS)	7	8	29	33	6	2	38	13
Phosphatidyl ethanolamine (PE)	16	3	20	17	10	1	39	9
Phosphatidylglycerol (PG)	9	13	22	29	0	0	13	21
Phosphatidylinositol (PI)	6	17	23	44	1	3	3	12
Ceramides (cer)	6	0	6	6	0	0	5	5
Sphingomyelin (SM)	37	0	17	62	6	2	47	14
Sterol (ST)	13	0	23	21	7	2	12	16
Cholesterol ester (CE)	3	0	4	2	1	0	1	2

3.3. Physiological parameters of *D. magna* exposed to MaE

MaE-exposed *Daphnia* exhibited numerous physiological changes relative to control populations. For example, cholesterol content significantly increased in *D. magna* in both MaE treatments after 48 and 96 h; as well, the two MaE treatments differed after 96 h exposure (Fig. 4A, $P < 0.05$). E2H activity and ecdysone content also significantly increased in both MaE treatments (Fig. 4B&C, $P < 0.05$). Activity of CYP314A1 and 20E content differed between MaE treatments after 48 h exposure (Fig. 4D&E, $P < 0.05$). MaE treatments also significantly increased activities of ecdysone receptor and retinoic acid X receptor relative to the control, with the high MaE treatment having greater effects than the low MaE treatment after both 48 and 9 h (Fig. 4F&G, $P < 0.05$).

MaE significantly increased activity of FAMEt and amount of juvenile hormone after 96 h of exposure (Fig. 4H&I, $P < 0.05$). There was a strong concentration effect on the activity of the steroid receptor

coactivator, and both MaE treatments were higher than corresponding controls (Fig. 4J, $P < 0.05$).

We observed that activity of SREBP protein was significantly higher relative to the control after 48 h in the high density MaE treatment, whereas both MaE treatments exhibited enhanced activity after 96 h exposure (Fig. 4K, $P < 0.05$). ACC and DGAT activity were significantly increased in both MaE treatments, while exposure time was also significant (Fig. 4L&M, $P < 0.05$). Finally, TAG content in *D. magna* was significantly increased in both MaE treatments (Fig. 4N, $P < 0.05$), with the higher concentration exhibiting the greatest increases.

3.4. Gene expression of *D. magna* exposed to MaE

MaE had strong but complex effects on regulation of key genes in *D. magna* (Fig. 5). Transcription of *Neverland*, *ECR*, *HR3*, *Met* and *SRC* genes all changed significantly following 48 h exposure. The high density MaE treatment experienced significantly higher expression of the

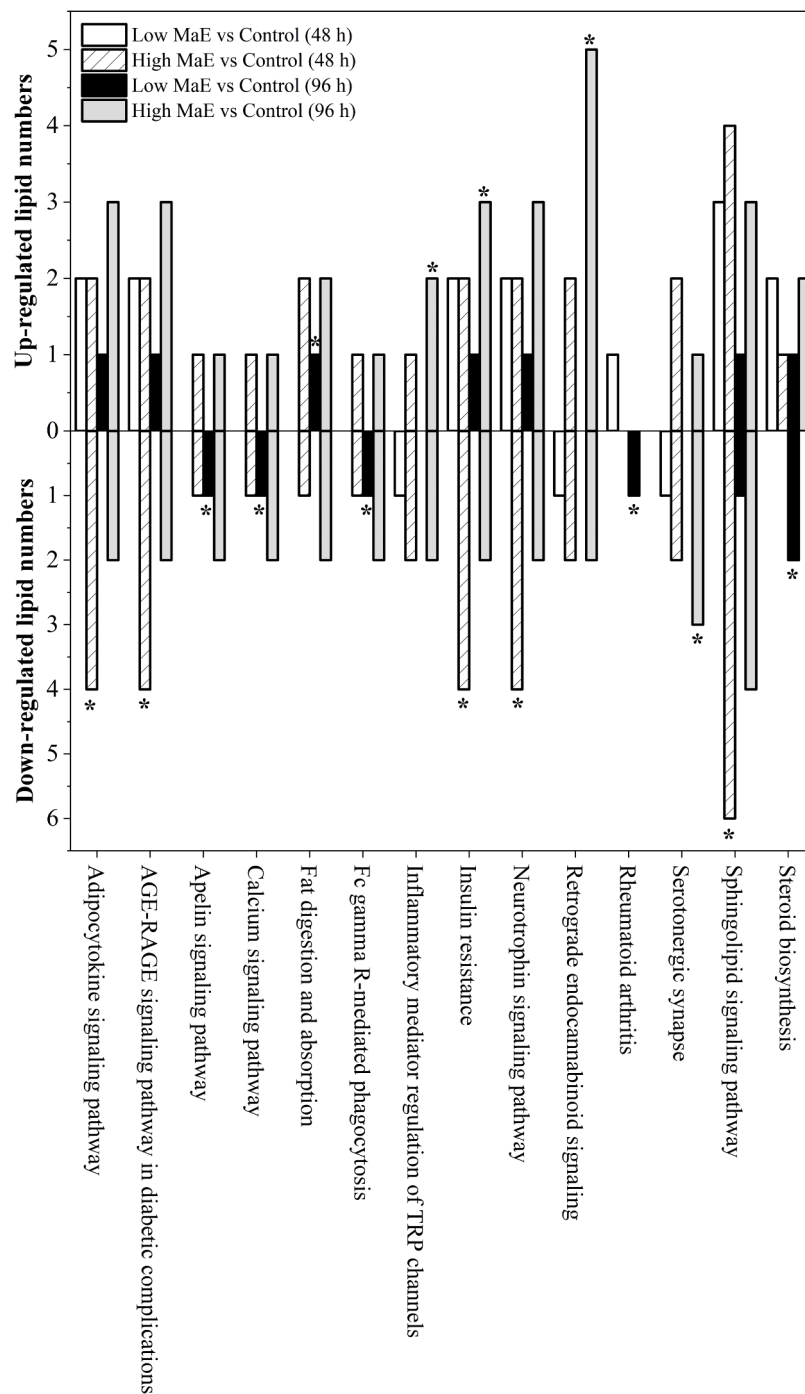


Fig. 3. Significantly enriched KEGG pathway in *D. magna* after acute exposure to MaE based on lipid metabolites (n = 3). Metabolites that were not down- or up-regulated are not shown.

Neverland gene relative to controls, while those of *ECR*, *HR3*, *Met* and *SRC* genes increased in the low density MaE treatment ($P < 0.05$). However, after 96 h exposure, we observed no significant difference in transcription of any of these genes between treatments and the control ($P > 0.05$, Fig. 5). We also observed up-regulation within 48 h of exposure of *RXR*, *SREBP-1* and *DGAT-1* in MaE treatments relative to the control ($P < 0.05$). However, as the exposure time increased to 96 h, the aforementioned genes were up-regulated only in the high density MaE treatment. After 48 h exposure, *Hb2* gene expression significantly increased in both MaE treatments ($P < 0.05$), though this result was reversed after 96 h exposure in the high density MaE treatment. ($P < 0.05$).

3.5. Growth and reproduction in *D. magna* exposed to MaE

Relative to the control (Fig. 6A), the high density MaE treatment produced 45.7 % more of the earliest eggs per *D. magna* adult (Fig. 6A and Table S2, $P < 0.05$), whereas reproduction was not elevated in the low density MaE treatment ($P > 0.05$). Primiparous females commenced newborn production significantly earlier in both MaE treatments relative to the control, and newborns were larger than those in the control (Fig. 6B). Total offspring number in both MaE treatments also increased, though only the high density MaE treatment differed from the control (increased by 30.6 %; Fig. 6C and Table S2, $P < 0.05$). Adult female body length of *D. magna* increased significantly in both MaE treatments at

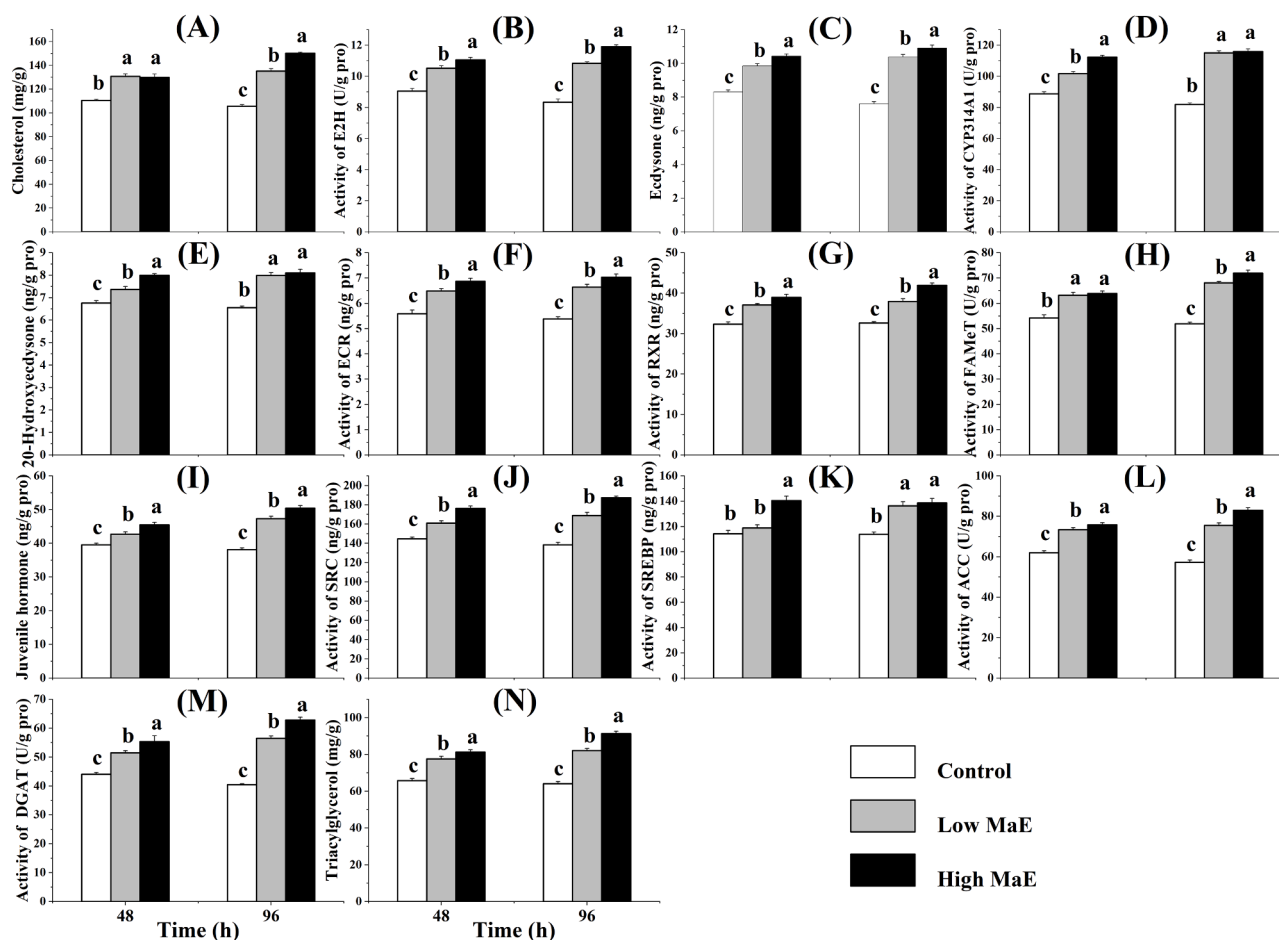


Fig. 4. Mean (\pm SD; $n = 4$) physiological parameters of triacylglycerol synthesis in *D. magna* exposed to MaE for 48 h or 96 h (A) Cholesterol, (B) E2H: ecdysterone 2-hydroxylase, (C) Ecdysone, (D) CYP314A1: ecdysone 20-monooxygenase, (E) 20E: 20-hydroxyecdysone, (F) ECR: ecdysone receptor, (G) RXR: retinoic acid X receptor, (H) FAMEt: farnesic acid methyltransferase, (I) Juvenile hormone, (J) SRC: steroid receptor coactivator, (K) SREBP: sterol regulatory element binding protein, (L) ACC: acetyl-CoA carboxylase, (M) DGAT: diacylglycerol transferase, (N) TAG: triacylglycerol. Different letters on grouped bars indicate significant differences between the treatments using one-way ANOVA (Tukey HSD, $P < 0.05$).

each investigated time, ranging between +7.7 % to +33.6 % on days 7 and 21, respectively (Fig. 6D and Table S2, $P < 0.05$). Animals in the high density MaE treatment were significantly longer than those in the low density treatment on day 7 ($P < 0.05$).

3.6. TAG in MaE and its correlation to *Daphnia* lipid accumulation

Among the three selected lipid species of TAG, concentrations of trilaurin and tritradecanoin were less than 1 ng/mL in both MaE treatments (Table 2). However, GTS was present at 2.74 and 3.74 ng/mL in the low and high density MaE treatments, respectively, while it was detected in intracellular compounds of *M. aeruginosa* with a concentration of 2.15 ng/mL at 8×10^6 cells/mL, too. We observed significant positive correlations between GTS content of MaE and contents of cholesterol (96 h), TAG (48 & 96 h), and ecdysone (48 h) and juvenile hormone (96 h) in *D. magna* (Fig. 7).

We found Iso1-GTS and Iso2-GTS isomers of GTS in *D. magna* by searching the chemical formula ($C_{57}H_{110}O_6$) in *D. magna*'s lipid metabolites and determined that only the former was up-regulated by both low and high density MaE treatments at 48 h (Table S3). We detected positive correlations between Iso1-GTS and cholesterol, TAG and lipid accumulation, as well as all parameters involved in growth and reproduction of *D. magna* (Fig. 7). Also, we observed significant positive correlations among contents of cholesterol (96 h), TAG and lipid accumulation as well as growth and offspring size of exposed *D. magna* (Fig. 7).

4. Discussion

4.1. *M. aeruginosa* exudates alter lipid metabolism in *D. magna*

In this study, we demonstrated pronounced disruption of lipid metabolism associated with MaE exposure that affected *Daphnia* physiological and molecular characteristics. In addition, we detected TAG lipid species from MaE. TAG as an important energy storage fat is important to growth and development of *D. magna* (Jordão et al., 2016b). Fatty acids can be synthesized from acetyl coenzyme A and converted to diacylglycerols, which are then transported to other tissues via lipid transport. When fatty acids concentrations are too high, diacylglycerols are converted to TAG (Palm et al., 2012). TAG can also be synthesized by copper triphosphate perphosphatidic acid or by acylation of diacylglycerols (Canavoso et al., 2001). In addition, *de novo* formation of fat involves conversion of carbohydrates and proteins to fatty acids, which can be transferred from glycerol-3-phosphate acyltransferase to glycerotriphosphate (Holtorf et al., 2019). Lysophosphatidic acid from glycerotriphosphate can be catalyzed by 1-acylglycerol-3-phosphate acyltransferase in the second acyltransferase reaction (Takeuchi and Reue, 2009). Then, diacylglycerol can be dephosphorylated to generate TAG, which could be metabolized to phosphatidylinositol. Diacylglycerol can also produce phosphatidylcholine and phosphatidylethanolamine under the action of carnitine palmitoyl transferase and ethanolamine phosphate transferase, and these two lipids can be further converted into phosphatidylserine; these glycerol phospholipids make

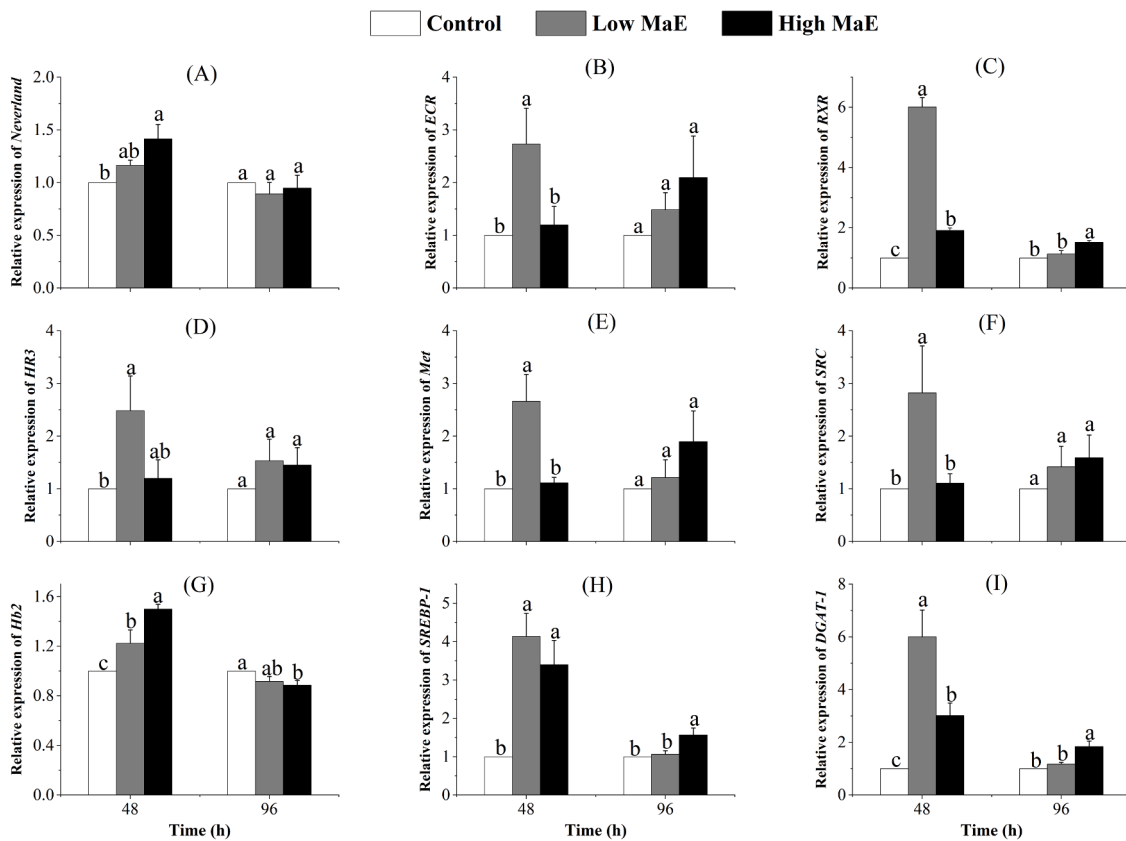


Fig. 5. Mean (\pm SD; $n = 4$) relative mRNA expression of nine genes involved in reproductive hormone signaling pathways (*Neverland*, *ECR*, *RXR*, *HR3*, *Met*, *SRC*, *Hb2*, *SREBP-1* and *DGAT-1*) after acute exposure of *D. magna* to MaE at different cell densities. Different letters on grouped bars indicate significant differences between the treatments using one-way ANOVA (Tukey HSD, $P < 0.05$).

important contributions to cell growth (Liu et al., 2014). Collectively, our results show that MaE induced fat accumulation in *D. magna* via increased production of lipid droplets, and also altered lipid components, especially elevated TAG (Fig. 4N).

Our KEGG pathway analysis revealed that MaE from low cell density culture induced down-regulation of sphingolipid metabolism pathway, the calcium metabolism pathway, and sterol synthesis, but up-regulation of fat cell digestion and the absorption metabolism pathway (Fig. 3). Calcium signaling pathway is closely related to lipid metabolism (Arruda et al., 2017). In *Drosophila melanogaster*, decreased Ca^{2+} levels resulted in increased fat storage (Toprak et al., 2020). In addition, sphingomyelin plays an important role in the sphingomyelin metabolic pathway. Sphingolipid metabolism is down-regulated by exposure to MaE, resulting in an increase in sphingomyelin. Previous studies have found that adding sphingomyelin to cells can increase cholesterol synthesis (Simons and Ikonen, 2000), which also is consistent with our study (Fig. 4A). Our high MaE treatment induced down-regulation of the neurotrophin signaling pathway, the adipocytokine signaling pathway, the AGE-RAGE signaling pathway, and the insulin resistance pathway. Advanced glycation products (AGEs) are a modified molecule formed by non-enzymatic reaction between aldehyde group of reducing sugar and lipid (Wang et al., 2020). The insulin metabolic pathway can inhibit lipolysis and promote fatty acid synthesis (Saltiel and Kahn, 2001; Wong and Sul, 2010), which is consistent with the verification results of our q-PCR experiment (Fig. 5). During the 96 h exposure time, high MaE treatment up-regulated inflammatory mediator regulation of TRP channels and retrograde endocannabinoid signaling. It also induced the down-regulation of serotonergic synapses signaling pathway. Retrograde endocannabinoid are active lipids, which can mediate the transport of arachidonic acid and other lipids (Haj-Dahmane et al., 2018). Arachidonic acid (AA) is an essential

polyunsaturated fatty acid required for normal growth and reproduction of *Daphnia* (Hartwich et al., 2012). Inflammation and viral infection can also lead to cellular lipid metabolism disorders, resulting in significant increases in intracellular lipid and cholesterol levels (Wipperman et al., 2014). In addition, some studies have found that 5-HT synaptic signaling pathway can induce lipid decomposition (Schlotz et al., 2012), and the down-regulation of this pathway indicates that fat decomposition is inhibited, which may lead to lipid accumulation. Our results highlight that MaE can interfere with lipid metabolism by affecting numerous endocrine pathways.

4.2. *M. aeruginosa* exudates induce lipid accumulation of *D. magna* via ecdysone and juvenile hormone signaling pathways

Ecdysone and juvenile hormone signaling pathways and retinoic acid X receptor (RXR) are involved in regulating lipid accumulation, homeostasis of neutral lipids (Jordão et al., 2016a), as well as TAG dynamics (Jordão et al., 2015).

Cholesterol is an important neutral lipid and the source of ecdysone metabolism (Miyakawa et al., 2018; Qu et al., 2018). The *Neverland* gene is located upstream of the ecdysone signaling pathway, and encodes cholesterol dehydrogenase, which plays an important role in cholesterol transport and metabolism (Rewitz and Gilbert, 2008; Rewitz et al., 2007). The increased cholesterol content and up-regulation of *Neverland* gene confirmed that MaE activated the ecdysone signaling pathway (Fig. 4A& 5A). In *D. magna*, ecdysone is not the final form binding to ecdysone receptor (ECR), but is instead converted to the final active substance, 20-hydroxyecdysone (20E) (Sumiya et al., 2014). When 20E binds to ECR, it forms heterodimer with RXR (Thomas et al., 1993). The nuclear receptor RXR could bind to ECR to form an RXR-ECR complex as a transcription factor (Miyakawa et al., 2018). We observed that after

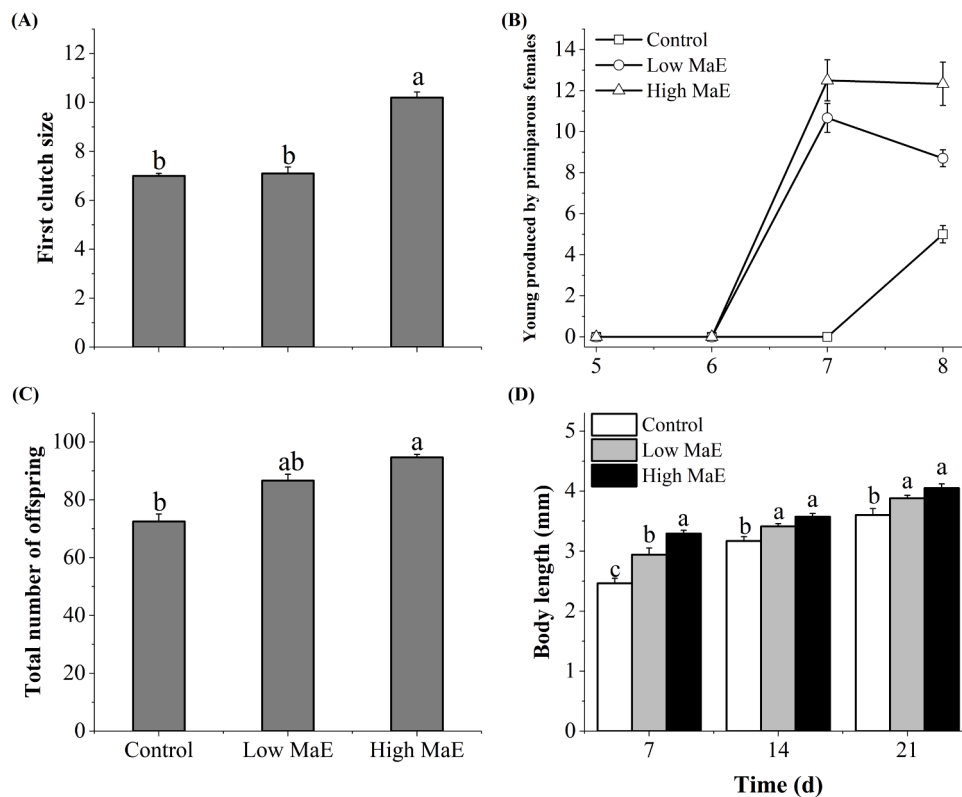


Fig. 6. Reproductive and growth parameters of *D. magna* during a 21-day MaE exposure experiment. Number of eggs produced (A) and (B) young produced per primiparous female on days 6, 7 or 8; (C) Total number of offspring per female after 21 days; (D) Body length of adult females on the 7th, 14th and 21st days (mean \pm SD; n = 10). Different letters on the grouped bars indicate significant differences between the treatments using one-way ANOVA (Tukey HSD, $P < 0.05$).

Table 2

Concentrations of TAG lipid species in different MaE solutions ($\text{ng}\cdot\text{mL}^{-1}$; mean \pm SD, n = 6).

Name	CAS No.	Formula	MaE of 2×10^4 cells/mL	MaE of 4×10^5 cells/mL	MaE of 8×10^6 cells/mL	Intracellular compounds of 8×10^6 cells/mL
Trilaurin	538-24-9	$\text{C}_{39}\text{H}_{74}\text{O}_6$	0.21 ± 0.24	0.15 ± 0.06	0.16 ± 0.08	0.09 ± 0.04
Glycerol tristearate (GTS)	555-43-1	$\text{C}_{57}\text{H}_{110}\text{O}_6$	2.74 ± 0.32	3.74 ± 0.44	3.19 ± 0.33	2.15 ± 0.12
Tritetradecanoin	555-45-3	$\text{C}_{45}\text{H}_{86}\text{O}_6$	0.019 ± 0.008	0.047 ± 0.021	0.021 ± 0.012	0.015 ± 0.007

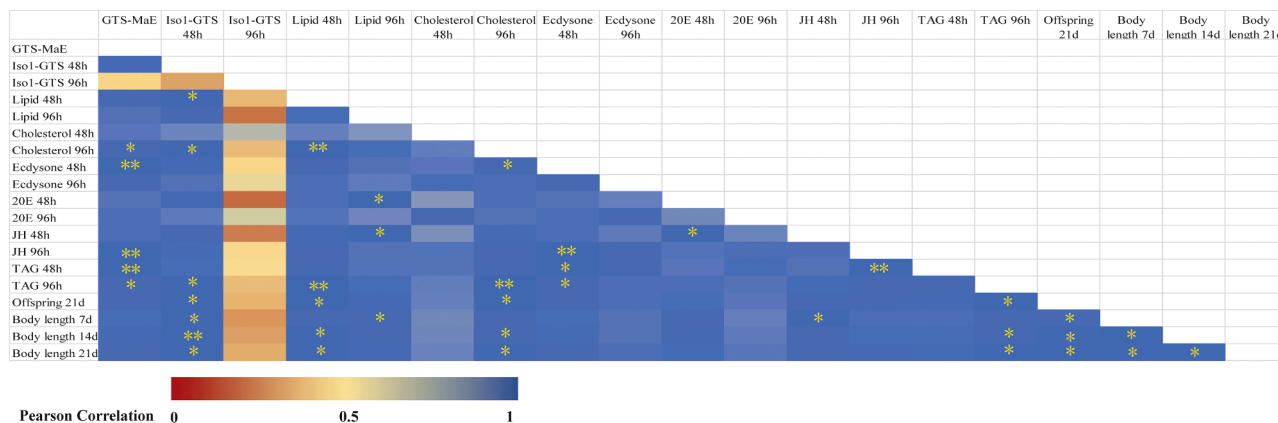


Fig. 7. Heatmap of Pearson's product moment correlations between tested parameters using all treatments and control data. Except GTS of MaE in the 2nd line and the 2nd column, other parameters are from *D. magna*. Asterisk indicates a significant correlation between the two parameters (*, $P < 0.05$; **, $P < 0.01$).

exposure to MaE, activities of E2H, CYP314A1, ECR and RXR, and the contents of ecdysone and 20E were enhanced (Fig. 4B–G). Our gene expression data highlighted that MaE treatment up-regulated the *HR3* gene in *D. magna* (Fig. 5). *HR3* is an ecdysone-induced gene in this species (Hannas and LeBlanc, 2010), encoding the ecdysone response transcription factor and regulation of expression of the sterol carrier protein 2 (SCP2). In addition, expression of the *ECR* gene encoding ecdysone receptor, the *RXR* gene encoding nuclear receptor RXR were also up-regulated after exposure to MaE (Fig. 5). These results highlight that MaE at both low and high concentration can activate the ecdysone signaling pathway in *D. magna*.

We also observed that FAMEt activity, juvenile hormone content, and steroid receptor coactivator activity and RXR activity all increased following exposure to MaE (Fig. 4). *Met* and *SRC* genes were up-regulated after 96 h of MaE exposure, and *Hb2* gene was also up-regulated after 48 h of MaE exposure (Fig. 5). These results are consistent with the observed elevated transcription of *Met*, *SRC* and *Hb2* genes after exposure to juvenile hormone analogues (Jordão et al., 2016a).

Sterol regulatory element binding protein (SREBP) transcription factor can activate the de novo lipogenesis (DNL) pathway in invertebrates (Ameer et al., 2014). In the DNL pathway, ACC is involved in the formation of palmitic acid (PA) for the synthesis of polyunsaturated fatty acids. In this study, activities of SREBP and ACC increased after *D. magna* was acutely exposed to MaE (Figure 4K&L). In addition, activity of diacylglycerol transferase (DGAT) involved in the conversion of fatty acids from glycerol triphosphate (G-3-P) to TAG also increased (Fig. 4M). We also found that the *SREBP-1* gene and the *DGAT-1* gene were both up-regulated after MaE exposure (Fig. 5). Collectively, these results show that MaE can further induce synthesis of TAG by activating the reproductive hormone signaling pathway.

4.3. Consequences of obesogen effects caused by *M. aeruginosa*

Usually, *D. magna* accumulates lipids before reproduction and allocates more energy to reproduction than to growth during spawning (Nogueira et al., 2004). This means that changes to lipid storage in females can alter future reproduction. We observed that MaE changed fat storage in adult female *D. magna* and increased their production of cholesterol and TAG (Fig. 4A&N). The first clutch of eggs in primiparous *D. magna* increased in the high density MaE treatment (Fig. 6A), while the date of release of initial newborns was advanced relative to that of controls (Fig. 6B). However, daphnids treated with low density MaE generated fewer eggs and offspring than the high MaE treatment, possibly because this treatment provided less lipid analogues to reproductive females.

Our study also found that signaling pathways of ecdysone and juvenile hormone in *D. magna* were affected by MaE, providing new evidence for their role in connecting lipid metabolism and reproduction. 20-hydroxyecdysone increases lipid accumulation and reproduction in *D. magna* (Sumiya et al., 2014), which is consistent with our results. We found that MaE activated the juvenile hormone signaling pathway and increased body length of *D. magna*, especially in the early stage of development (the 7th day; Fig. 6D). We also observed that the total number of offspring produced by *D. magna* exposed to MaE from the high density treatment increased significantly (Fig. 6C).

Evidence for increased TAG production in *D. magna* is provided by more up- than down-regulated metabolites in both MaE treatments (Table 1), and by the quantification of TAG content with ELISA (Fig. 4N). Polyunsaturated fatty acids are involved in TAG accumulation and are extremely important for growth and development of *D. magna* (Taipale et al., 2011). A large number of long-chain polyunsaturated fatty acids were distributed to eggs in *D. magna* at the early reproductive stage (Wacker and Martin-Creuzburg, 2007). On the other hand, female *D. magna* accumulate massive glycerolipids and glycerophospholipids from food to generate eggs. We observed high MaE treatment induced more up- than down-regulated sphingolipids, which are transferred to

developing offspring (Sengupta et al., 2017). Thus, MaE might promote egg production of *D. magna* by increasing TAG, glycerolipids and sphingolipids storage. The presence of GTS in MaE in our study provides evidence of a correlation between lipid species released by *M. aeruginosa* cells and lipid accumulation in daphnids (Fig. 7 & Table 2). If cyanobacteria release such lipids during the bloom season in nature, it could be risky for aquatic animals that are exposed to these potential exogenous obesogens. More research is needed to identify specific chemicals responsible and reveal the pathways of their biosynthesis in cyanobacterial cells.

Our study demonstrated that a dominant species of cyanobacteria can release bioactive chemicals that induce disordered lipid metabolism and enhanced reproduction in the common and important zooplankton species, *D. magna*. These effects may induce a stronger top-down effect on phytoplankton, particularly on edible algal species (Ger et al., 2018; Solis et al., 2018). As such, cyanobacteria would potentially benefit by enhancing abundance of their competitor's predator. Previous work observed that carp fed with *Microcystis* for 28 days experienced elevated size and number of lipid droplets in liver (Li et al., 2004). The fat metabolism disorder caused by *M. aeruginosa* in this study has the potential to induce complex direct and indirect changes to aquatic ecosystems.

5. Conclusions

Two concentrations of *M. aeruginosa* exudates significantly increased body length and reproduction of *D. magna*, including spawning and total number of young produced. MaE induced transcription of the RXR receptor, activated signaling pathways of ecdysone and juvenile hormone, improved the activity of steroid regulatory element binding protein, and promoted synthesis of TAG. MaE also affected other endocrine and neural signaling pathways, which further interfered with lipid metabolism. Increased lipid droplets and some lipid metabolites, including cholesterol and TAG, were in turn allocated to enhanced reproduction in MaE-exposed daphnids. Glycerolipids and glycerophospholipids metabolites were up-regulated for reproduction and the formation of the new carapace. In addition, detection of GTS from MaE in this study may spawn future research not only to reveal the mechanism of GTS biosynthesis by cyanobacteria but also to investigate its distribution in water during bloom periods, as well as to test the quality of offspring in subsequent generations. This study provides insights into novel risks of cyanobacterial blooms via obesogenic effects.

CRedit authorship contribution statement

Jinlong Zhang: Writing – original draft, Software, Methodology, Investigation, Formal analysis, Data curation, Conceptualization. **Xuexiu Chang:** Writing – review & editing, Supervision, Funding acquisition. **Hugh J. MacIsaac:** Writing – review & editing. **Yuan Zhou:** Writing – original draft, Validation, Methodology, Investigation. **Daochun Xu:** Visualization, Validation, Investigation. **Jingjing Li:** Software, Methodology. **Jun Xu:** Software, Methodology. **Tao Wang:** Software, Methodology. **Hongyan Zhang:** Validation, Investigation. **Zimeng Peng:** Visualization. **Jiayao Wen:** Software, Methodology. **Runbing Xu:** Writing – review & editing, Visualization, Supervision, Resources, Project administration, Funding acquisition, Conceptualization.

Declaration of competing interest

The authors declare the following financial interests/personal relationships which may be considered as potential competing interests:

Runbing Xu reports financial support was provided by National Natural Science Foundation of China. Xuexiu Chang reports financial support was provided by National Natural Science Foundation of China. Runbing Xu reports financial support was provided by Yunnan Applied

Basic Research Project. Xuexiu Chang reports financial support was provided by Yunnan Applied Basic Research Project. Xuexiu Chang reports financial support was provided by Yunnan Provincial Department of Education Science Research Fund Project. Xuexiu Chang reports financial support was provided by Natural Sciences and Engineering Research Council of Canada. Hugh J. MacIsaac reports financial support was provided by Natural Sciences and Engineering Research Council of Canada. Hugh J. MacIsaac reports financial support was provided by Canada research chair. If there are other authors, they declare that they have no known competing financial interests or personal relationships that could have appeared to influence the work reported in this paper.

Acknowledgements

This research was supported by National Natural Science Foundation of China (No. 32260318, U1902202, U2102216 and 31800433), Yunnan Applied Basic Research Projects (Nos. 202201AT070093, 202101AU070133 and 2019FA043), the International Joint Innovation Team for Yunnan Plateau Lakes and Laurentian Great Lakes and Yunnan Collaborative Innovation Center for Plateau Lake Ecology and Environmental Health to XC, and an NSERC Discovery grant and Canada Research Chair to HJM.

Supplementary materials

Supplementary material associated with this article can be found, in the online version, at [doi:10.1016/j.hal.2024.102790](https://doi.org/10.1016/j.hal.2024.102790).

Data availability

Data will be made available on request.

References

- Ameer, F., Scanduzzi, L., Hasnain, S., Kalbacher, H., Zaidi, N., 2014. *De novo* lipogenesis in health and disease. *Metabolism* 63, 895–902. <https://doi.org/10.1016/j.metabol.2014.04.003>.
- Arruda, A., Pers, B., Parlakgul, G., Güney, E., Goh, T., Cagampan, E., Lee, G., Goncalves, R., Hotamisligil, G., 2017. Defective STIM-mediated store operated Ca²⁺ entry in hepatocytes leads to metabolic dysfunction in obesity. *Elife* 6, 29968. <https://doi.org/10.7554/eLife.29968>.
- Baillie-Hamilton, P.F., 2002. Chemical toxins: a hypothesis to explain the global obesity epidemic. *J. Altern. Complement. Med.* 8, 185–192. <https://doi.org/10.1089/107555302317371479>.
- Canavoso, L.E., Jouni, Z.E., Karnas, K.J., Pennington, J.E., Wells, M.A., 2001. Fat metabolism in insects. *Annu. Rev. Nutr.* 21, 23–46. <https://doi.org/10.1146/annurev.nutr.21.1.23>.
- Catala, A., 2013. Five decades with polyunsaturated fatty acids: chemical synthesis, enzymatic formation, lipid peroxidation and its biological effects. *J. Lipids*, 710290. <https://doi.org/10.1155/2013/710290>, 2013.
- Chen, W., Dou, J., Xu, X., Ma, X., Chen, J., Liu, X., 2024. β -cyclocitral, a novel AChE inhibitor, contributes to the defense of *Microcystis aeruginosa* against *Daphnia* grazing. *J. Hazard. Mater.* 465, 133248. <https://doi.org/10.1016/j.jhazmat.2023.133248>.
- De Meester, L., Declerck, S.A.J., Ger, K.A., 2023. Beyond *Daphnia*: a plea for a more inclusive and unifying approach to freshwater zooplankton ecology. *Hydrobiologia* 850, 4693–4703. <https://doi.org/10.1007/s10750-023-05217-3>.
- DeMott, W.R., Gulati, R.D., Van Donk, E., 2001. *Daphnia* food limitation in three hypereutrophic Dutch lakes: evidence for exclusion of large-bodied species by interfering filaments of cyanobacteria. *Limnol. Oceanogr.* 46, 2054–2060. <https://doi.org/10.4319/lo.2001.46.8.2054>.
- DeMott, W.R., Zhang, Q.-X., Carmichael, W.W., 1991. Effects of toxic cyanobacteria and purified toxins on the survival and feeding of a copepod and three species of *Daphnia*. *Limnol. Oceanogr.* 36, 1346–1357. <https://doi.org/10.4319/lo.1991.36.7.1346>.
- Dickman, E.M., Newell, J.M., González, M.J., Vanni, M.J., 2008. Light, nutrients, and food-chain length constrain planktonic energy transfer efficiency across multiple trophic levels. *Proc. Natl Acad. Sci.* 105, 18408–18412. <https://doi.org/10.1073/pnas.0805566105>.
- Flaherty, C.M., Dodson, S.I., 2005. Effects of pharmaceuticals on *Daphnia* survival, growth, and reproduction. *Chemosphere* 61, 200–207. <https://doi.org/10.1016/j.chemosphere.2005.02.016>.
- Fuertes, I., Jordao, R., Casas, F., Barata, C., 2018. Allocation of glycerolipids and glycerophospholipids from adults to eggs in *Daphnia magna*: perturbations by compounds that enhance lipid droplet accumulation. *Environ. Pollut.* 242, 1702–1710. <https://doi.org/10.1016/j.envpol.2018.07.102>.
- Fuertes, I., Jordao, R., Pina, B., Barata, C., 2019. Time-dependent transcriptomic responses of *Daphnia magna* exposed to metabolic disruptors that enhanced storage lipid accumulation. *Environ. Pollut.* 249, 99–108. <https://doi.org/10.1016/j.envpol.2019.02.102>.
- Fuertes, I., Piña, B., Barata, C., 2020. Changes in lipid profiles in *Daphnia magna* individuals exposed to low environmental levels of neuroactive pharmaceuticals. *Sci. Total. Environ.* 733, 139029. <https://doi.org/10.1016/j.scitotenv.2020.139029>.
- Ger, K.A., Naus-Wiezer, S., De Meester, L., Lürling, M., 2018. Zooplankton grazing selectivity regulates herbivory and dominance of toxic phytoplankton over multiple prey generations. *Limnol. Oceanogr.* 64, 1214–1227. <https://doi.org/10.1002/lno.11108>.
- Ger, K.A., Urrutia-Cordero, P., Frost, P.C., Hansson, L.-A., Sarnelle, O., Wilson, A.E., Lürling, M., 2016. The interaction between cyanobacteria and zooplankton in a more eutrophic world. *Harmful Algae* 54, 128–144. <https://doi.org/10.1016/j.hal.2015.12.005>.
- Grün, F., Blumberg, B., 2009. Endocrine disruptors as obesogens. *Mol. Cell Endocrinol.* 304, 19–29. <https://doi.org/10.1016/j.mce.2009.02.018>.
- Haj-Dahmane, S., Shen, R.-Y., Elmes, M.W., Studholme, K., Kanjiya, M.P., Bogdan, D., Thanos, P.K., Miyauchi, J.T., Tsirka, S.E., Deutsch, D.G., Kaczocha, M., 2018. Fatty acid-binding protein 5 controls retrograde endocannabinoid signaling at central glutamate synapses. *Proc. Natl Acad. Sci. U S A* 115, 3482–3487. <https://doi.org/10.1073/pnas.1721339115>.
- Hannas, B.R., LeBlanc, G.A., 2010. Expression and ecdysteroid responsiveness of the nuclear receptors HR3 and E75 in the crustacean *Daphnia magna*. *Mol. Cell Endocrinol.* 315, 208–218. <https://doi.org/10.1016/j.mce.2009.07.013>.
- Hartwich, M., Martin-Creuzburg, D., Rothhaupt, K.-O., Wacker, A., 2012. Oligotrophication of a large, deep lake alters food quantity and quality constraints at the primary producer–consumer interface. *Oikos* 121, 1702–1712. <https://doi.org/10.1111/j.1600-0706.2011.20461.x>.
- Ho, J.C., Michalak, A.M., Pahlevan, N., 2019. Widespread global increase in intense lake phytoplankton blooms since the 1980s. *Nature* 574, 667–670. <https://doi.org/10.1038/s41586-019-1648-7>.
- Holtf, M., Lenaerts, C., Cullen, D., Vanden Broeck, J., 2019. Extracellular nutrient digestion and absorption in the insect gut. *Cell Tissue Res.* 377, 397–414. <https://doi.org/10.1007/s00441-019-03031-9>.
- Huisman, J., Codd, G.A., Paerl, H.W., Ibelings, B.W., Verspagen, J.M.H., Visser, P.M., 2018. Cyanobacterial blooms. *Nat. Rev. Microbiol.* 16, 471–483. <https://doi.org/10.1038/s41579-018-0040-1>.
- Jones, M.R., Pinto, E., Torres, M.A., Dórr, F., Mazur-Marzec, H., Szubert, K., Tartaglione, L., Dell’Aversano, C., Miles, C.O., Beach, D.G., McCarron, P., Sivonen, K., Fewer, D.P., Jokela, J., Janssen, E.M.L., 2021. CyanoMetDB, a comprehensive public database of secondary metabolites from cyanobacteria. *Water Res.* 196, 117017. <https://doi.org/10.1016/j.watres.2021.117017>.
- Jordão, R., Campos, B., Piña, B., Tauler, R., Soares, A.M.V.M., Barata, C., 2016a. Mechanisms of action of compounds that enhance storage lipid accumulation in *Daphnia magna*. *Environ. Sci. Technol.* 50, 13565–13573. <https://doi.org/10.1021/acs.est.6b04768>.
- Jordão, R., Casas, J., Fabrias, G., Campos, B., Piña, B., Lemos Marco, F.L., Soares Amadeu, M.V.M., Tauler, R., Barata, C., 2015. Obesogens beyond vertebrates: lipid perturbation by tributyltin in the Crustacean *Daphnia magna*. *Environ. Health Persp.* 123, 813–819. <https://doi.org/10.1289/ehp.1409163>.
- Jordão, R., Garreta, E., Campos, B., Lemos, M.F.L., Soares, A.M.V.M., Tauler, R., Barata, C., 2016b. Compounds altering fat storage in *Daphnia magna*. *Sci. Total. Environ.* 545–546, 127–136. <https://doi.org/10.1016/j.scitotenv.2015.12.097>.
- Li, J., Chang, X., Zhao, S., Zhang, Y., Pu, Q., Wang, Y., Li, J., 2024. Exudates of *Microcystis aeruginosa* on oxidative stress and inflammatory responses in gills of *Sinocyclocheilus grahami*. *Ecotox. Environ. Safe* 280, 116587. <https://doi.org/10.1016/j.ecoenv.2024.116587>.
- Li, X.-Y., Chung, I.-K., Kim, J.-I., Lee, J.-A., 2004. Subchronic oral toxicity of microcystin in common carp (*Cyprinus carpio* L.) exposed to *Microcystis* under laboratory conditions. *Toxicol.* 44, 821–827.
- Liu, Y., Wang, W., Shui, G., Huang, X., 2014. CDP-diacylglycerol synthetase coordinates cell growth and fat storage through phosphatidylinositol metabolism and the insulin pathway. *PLoS Genet.* 10, e1004172. <https://doi.org/10.1371/journal.pgen.1004172>.
- Lürling, M., 2021. Grazing resistance in phytoplankton. *Hydrobiologia* 848, 237–249. <https://doi.org/10.1007/s10750-020-04370-3>.
- Lürling, M., van der Grinten, E., 2003. Life-history characteristics of *Daphnia* exposed to dissolved microcystin-LR and to the cyanobacterium *Microcystis aeruginosa* with and without microcystins. *Environ. Toxicol. Chem.* 22, 1281–1287. <https://doi.org/10.1002/etc.5620220614>.
- Lynn, D.A., Dalton, H.M., Sowa, J.N., Wang, M.C., Soukas, A.A., Curran, S.P., 2015. Omega-3 and -6 fatty acids allocate somatic and germline lipids to ensure fitness during nutrient and oxidative stress in *Caenorhabditis elegans*. *Proc. Natl Acad. Sci. U S A* 112, 15378–15383. <https://doi.org/10.1073/pnas.1514012112>.
- Miyakawa, H., Sato, T., Song, Y., Tollefsen, K.E., Iguchi, T., 2018. Ecdysteroid and juvenile hormone biosynthesis, receptors and their signaling in the freshwater microcrustacean *Daphnia*. *J. Steroid Biochem. Mol. Biol.* 184, 62–68. <https://doi.org/10.1016/j.jsbmb.2017.12.006>.
- Nogueira, A.J.A., Baird, D.J., Soares, A.M.V.M., 2004. Testing physiologically-based resource allocation rules in laboratory experiments with *Daphnia magna* Straus. *Annales De Limnologie - Int. J. Limnol.* 40, 257–267.
- Paerl, H.W., Huisman, J., 2008. Blooms like it hot. *Science* (1979) 320, 57–58. <https://doi.org/10.1126/science.1155398>.
- Palm, W., Sampaio, J., Brankatschk, M., Carvalho, M., Mahmoud, A., Shevchenko, A., Eaton, S., 2012. Lipoproteins in *Drosophila melanogaster*—assembly, function, and

- influence on tissue lipid composition. *PLoS Genet.* 8, e1002828. <https://doi.org/10.1371/journal.pgen.1002828>.
- Plaas, H.E., Paerl, H.W., 2021. Toxic cyanobacteria: a growing threat to water and air quality. *Environ. Sci. Technol.* 55, 44–64. <https://doi.org/10.1021/acs.est.0c06653>.
- Qu, Z., Bendena, W.G., Tobe, S.S., Hui, J.H.L., 2018. Juvenile hormone and sesquiterpenoids in arthropods: biosynthesis, signaling, and role of microRNA. *J. Steroid Biochem. Mol. Biol.* 184, 69–76. <https://doi.org/10.1016/j.jsmb.2018.01.013>.
- Rewitz, K.F., Gilbert, L.I., 2008. *Daphnia* Halloween genes that encode cytochrome P450s mediating the synthesis of the arthropod molting hormone: evolutionary implications. *BMC Evol. Biol.* 8, 60. <https://doi.org/10.1186/1471-2148-8-60>.
- Rewitz, K.F., O'Connor, M.B., Gilbert, L.I., 2007. Molecular evolution of the insect Halloween family of cytochrome P450s: Phylogeny, gene organization and functional conservation. *Insect. Biochem. Molec.* 37, 741–753. <https://doi.org/10.1016/j.ibmb.2007.02.012>.
- Saltiel, A.R., Kahn, C.R., 2001. Insulin signalling and the regulation of glucose and lipid metabolism. *Nature* 414, 799–806. <https://doi.org/10.1038/414799a>.
- Schlottz, N., Sørensen, J.G., Martin-Creuzburg, D., 2012. The potential of dietary polyunsaturated fatty acids to modulate eicosanoid synthesis and reproduction in *Daphnia magna*: a gene expression approach. *Compar. Biochem. Physiol. Part A Molec. Integr. Physiol.* 162, 449–454. <https://doi.org/10.1016/j.cbpa.2012.05.004>.
- Schmittgen, T.D., Livak, K.J., 2008. Analyzing real-time PCR data by the comparative CT method. *Nat. Protoc.* 3, 1101–1108. <https://doi.org/10.1038/nprot.2008.73>.
- Sengupta, N., Reardon, D., Gerard, P., Baldwin, W., 2017. Exchange of polar lipids from adults to neonates in *Daphnia magna*: perturbations in sphingomyelin allocation by dietary lipids and environmental toxicants. *PLoS One* 12, e0178131. <https://doi.org/10.1371/journal.pone.0178131>.
- Simons, K., Ikonen, E., 2000. How cells handle cholesterol. *Science* (1979) 290, 1721–1726. <https://doi.org/10.1126/science.290.5497.1721>.
- Solis, M., Pawlik-Skowrońska, B., Adamczuk, M., Kalinowska, R., 2018. Dynamics of small-sized Cladocera and their algal diet in lake with toxic cyanobacterial water blooms. *Ann. Limnol.-Int. J. Lim.* 54, 6.
- Sumiya, E., Ogino, Y., Miyakawa, H., Hiruta, C., Toyota, K., Miyagawa, S., 2014. Roles of ecdysteroids for progression of reproductive cycle in the fresh water crustacean *Daphnia magna*. *Front. Zool.* 11, 60. <https://doi.org/10.1186/s12983-014-0060-2>.
- Taipale, S.J., Kainz, M.J., Brett, M.T., 2011. Diet-switching experiments show rapid accumulation and preferential retention of highly unsaturated fatty acids in *Daphnia*. *Oikos*. 120, 1674–1682. <https://doi.org/10.1111/j.1600-0706.2011.19415.x>.
- Takeuchi, K., Reue, K., 2009. Biochemistry, physiology, and genetics of GPAT, AGPAT, and lipin enzymes in triglyceride synthesis. *Am. J. Physiol.-endoc. M* 296. <https://doi.org/10.1152/ajpendo.90958.2008>. E1195-E1209.
- Thomas, H.E., Stunnenberg, H.G., Stewart, A.F., 1993. Heterodimerization of the *Drosophila* ecdysone receptor with retinoid X receptor and ultraspiracle. *Nature* 362, 471–475. <https://doi.org/10.1038/362471a0>.
- Thomas, P.K., Kunze, C., Van de Waal, D.B., Hillebrand, H., Striebel, M., 2022. Elemental and biochemical nutrient limitation of zooplankton: A meta-analysis. *Ecol. Lett.* 25, 2776–2792. <https://doi.org/10.1111/ele.14125>.
- Toprak, U., Hegedus, D., Doğan, C., Güney, G., 2020. A journey into the world of insect lipid metabolism. *Arch. Insect. Biochem.* 104, e21682. <https://doi.org/10.1002/arch.21682>.
- Wacker, A., Martin-Creuzburg, D., 2007. Allocation of essential lipids in *Daphnia magna* during exposure to poor food quality. *Funct. Ecol.* 21, 738–747. <https://doi.org/10.1111/j.1365-2435.2007.01274.x>.
- Wang, T., Xu, D., Chang, X., Maclsaac, H.J., Li, J., Xu, J., Zhang, J., Zhang, H., Zhou, Y., Xu, R., 2024. Can a shift in dominant species of *Microcystis* alter growth and reproduction of waterfleas? *Harmful Algae* 136, 102657. <https://doi.org/10.1016/j.hal.2024.102657>.
- Wang, X., Liu, J., Yang, Y., Zhang, X., 2020. An update on the potential role of advanced glycation end products in glycolipid metabolism. *Life Sci.* 245, 117344. <https://doi.org/10.1016/j.lfs.2020.117344>.
- Wipperfman, M.F., Sampson, N.S., Thomas, S.T., 2014. Pathogen roid rage: cholesterol utilization by *Mycobacterium tuberculosis*. *Crit. Rev. Biochem. Mol.* 49, 269–293. <https://doi.org/10.3109/10409238.2014.895700>.
- Wong, R.H.F., Sul, H.S., 2010. Insulin signaling in fatty acid and fat synthesis: a transcriptional perspective. *Curr. Opin. Pharmacol.* 10, 684–691. <https://doi.org/10.1016/j.coph.2010.08.004>.
- Xu, R., Jiang, Y., Maclsaac, H.J., Chen, L., Li, J., Xu, J., Wang, T., Zi, Y., Chang, X., 2019. Blooming cyanobacteria alter water flea reproduction via exudates of estrogen analogues. *Sci. Total. Environ.* 696, 133909. <https://doi.org/10.1016/j.scitotenv.2019.133909>.
- Zhao, S., Chang, X., Li, J., Zhu, Y., Pan, X., Hua, Z., Li, J., 2023. The two-way immunotoxicity in native fish induced by exudates of *Microcystis aeruginosa*: immunostimulation and immunosuppression. *J. Hazard. Mater.*, 132554. <https://doi.org/10.1016/j.jhazmat.2023.132554>.
- Zhou, Y., Xu, J., Maclsaac, H.J., McKay, R.M., Xu, R., Pei, Y., Zi, Y., Li, J., Qian, Y., Chang, X., 2023. Comparative metabolomic analysis of exudates of microcystin-producing and microcystin-free *Microcystis aeruginosa* strains. *Front. Microbiol.* 13, 1075621. <https://doi.org/10.3389/fmicb.2022.1075621>.
- Zuo, Z., 2023. Emission of cyanobacterial volatile organic compounds and their roles in blooms. *Front. Microbiol.* 14. <https://doi.org/10.3389/fmicb.2023.1097712>.